WILEY | Hindawi

Research Article

H$_\infty$ Optimal Performance Design of an Unstable Plant under Bode Integral Constraint

Fanwei Meng ⬤,[1] Aiping Pang ⬤,[2] Xuefei Dong ⬤,[1] Chang Han ⬤,[1] and Xiaopeng Sha[1]

[1]*School of Control Engineering, Northeastern University at Qinhuangdao, Qinhuangdao 066004, China*
[2]*College of Electrical Engineering, Guizhou University, Guiyang 550025, China*

Correspondence should be addressed to Aiping Pang; 417524788@qq.com

This paper proposed the H$_\infty$ state feedback and H$_\infty$ output feedback design methods for unstable plants, which improved the original H$_\infty$ state feedback and H$_\infty$ output feedback. For the H$_\infty$ state feedback design of unstable plants, it presents the complete robustness constraint which is based on solving Riccati equation and Bode integral. For the H$_\infty$ output feedback design of unstable plants, the medium-frequency band should be considered in particular. Besides, this paper presents the method to select weight function or coefficients in the H$_\infty$ design, which employs Bode integral to optimize the H$_\infty$ design. It takes a magnetic levitation system as an example. The simulation results demonstrate that the optimal performance of perturbation suppression is obtained with the design of robustness constraint. The presented method is of benefit to the general H$_\infty$ design.

1. Introduction

Some constraints are often ignored in theory design so that the designed system could not been achieved [1]. The unstable poles should be considered in the design of unstable plants, which will have an impact on the system running [2]. For example, the performance index of fight aircraft is with a phase margin of 45° and however, the phase margin is 35° at last after lots of money is poured [3]. There is another type of unstable plants such as a magnetic levitation system, which has been built in some universities at home and abroad. But these systems could not run, and there exists a large peak in the data of sensitivity function [4]. And after X-29, the unstable poles are considered under the research on the Fight Aircraft JAS-39 and X-30, which succeeds. This paper solves the problem that it is how to make the control system obtained the optimal disturbance suppression.

There are two types of H$_\infty$ design, which are cycle formation based on coprime factorization, H$_\infty$ state feedback and H$_\infty$ output feedback such as DGKF [5, 6]. Cycle formation applies to control design of the flexible system

such as instances in [7]. This paper proposes H$_\infty$ state feedback and H$_\infty$ output feedback design together with the magnetic levitation system, which is applicable to unstable plants.

The key to achieve the H$_\infty$ control design is up to the weight function. The weight function is considered particularly for an unstable plant in H$_\infty$ control design. There are two different types of unstable plants. The first type is that the frequency band of mathematical model is 10 times larger than unstable mode, for example, in designing autopilot, the unstable mode is less than 1 rad/sec but the bandwidth is larger than 40 rad/sec [2, 8]. These systems will utilize the common H$_\infty$ design in general. The second type is that the unstable mode and the bandwidth of the closed-loop system are approximate, for example, in magnetic levitation systems in [9, 10], the unstable mode is 60~70 rad/sec and the bandwidth is 100 rad/sec. For the latter, there is obvious feature and it is to be considered in particular when using H$_\infty$ control design. This paper mainly discusses the second type of unstable plants, and the analysis results will benefit the explanation of the design of the first type.

2. Control Problem of Unstable Plants

In terms of control theory, there may be instability in control design for an unstable plant. Feedback characteristics must be considered in the design of the feedback system. Feedback systems have some performance such as robustness, sensitivity, and disturbance rejection, which can be changed only by feedback. The low sensitivity and disturbance rejection are the reasons why a system needs feedback control, but the robustness is essential performance in the feedback system. Therefore, the purpose of feedback control system design is to achieve low sensitivity and disturbance rejection.

2.1. Control System Performance Description. It is known that the sensitivity function describes the performance of the control system. The schematic of the feedback control system is shown in Figure 1, where K is the controller and G is the controlled plant. Then, its transfer function is given by

$$T = \frac{KG}{1 + KG}. \tag{1}$$

Define the sensitivity function S of the system as

$$S = \frac{d \ln T}{d \ln G} = \frac{dT/T}{dG/G}, \tag{2}$$

which shows the sensitivity function is the change of closed-loop function T with respect to the controlled plant. If the sensitivity of the designed system is low, it demonstrates that the designed system is robust to modeling error.

Taking derivative of (1) with respect to G and substituting into (2), the sensitivity function S is given by

$$S = \frac{G}{T} \frac{dT}{dG} = \frac{1}{1 + KG}, \tag{3}$$

which demonstrates the robustness and also other characteristics of the control system.

Figure 2 shows the Nyquist curve of a system, $K(j\omega)G(j\omega)$, and p is the minimum distance between KG and $(-1, j0)$, which can be obtained by

$$p = \min |1 + KG|. \tag{4}$$

Define the maximum peak of sensitivity as M_S,

$$M_S = \max |S(j\omega)| = \frac{1}{p}. \tag{5}$$

It is known that the response curve for open-loop systems is closer to the point $(-1, j0)$ as M_S is larger, which will make the system unstable while there is parameter perturbation of the plant G. The peak M_S is an index to robustness of the closed-loop system.

As is shown in Figure 3, the relation between sensitivity function and phase margin γ is formulated as

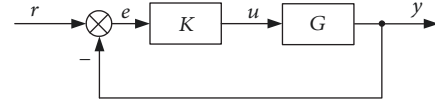$$\left| \frac{1}{S(j\omega)} \right| = |1 + KG| = 2 \left| \sin \frac{\gamma}{2} \right|. \tag{6}$$
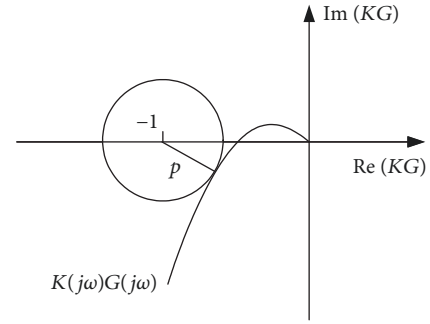

Figure 1: Feedback control system.

Figure 2: Nyquist curve of a system.
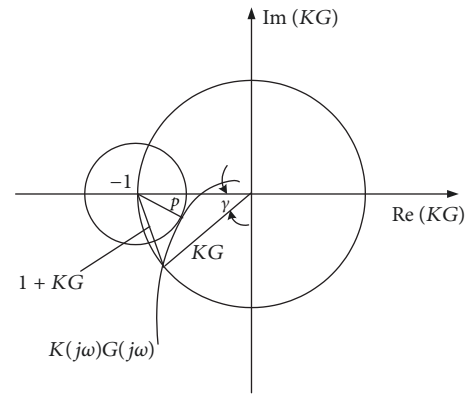

Figure 3: The relationship between phase margin γ and p.

The inequation can be obtained by

$$p \leq 2 \left| \sin \frac{\gamma}{2} \right|, \tag{7}$$

which shows that phase margin γ just decides the upper limit value but not the truth value of M_S. In fact, M_S may be very large and not robust while the system owns good phase margin and amplitude margin. Therefore, the maximum M_S of sensitivity is the real index reflecting the robustness of the system, which is often in the range of 1.2~2.0. If M_S in the designed system is 3, the system is unable to control [11, 12].

Equation (3) gives the method to measure the sensitivity. Figure 4 shows the systematic scheme with disturbance, and S can be seen as the transfer function from d to y. Equation (3) gives a method to measure the sensitivity. Figure 4 is the schematic with perturbation d, and S is the transfer function from d to y. The small S means that the output is not sensitive to perturbation, which is an important
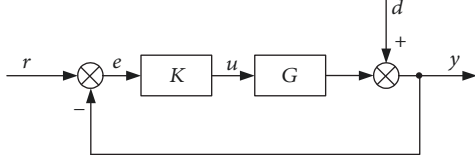
FIGURE 4: Suppression of output disturbance d.

characteristic of the feedback system. But it will enlarge the perturbation with $S > 1$.

As shown in Figure 4, the transfer function from reference input r to error signal e is the sensitivity,

$$\frac{E(s)}{R(s)} = \frac{1}{1 + KG} = S. \tag{8}$$

Then, the sensitivity reflects the ability of the system to track the input signal and smaller response to little error.

The sensitivity demonstrates that the effect of the system and the robustness could be reflected by its peak. The performance of the system is often reflected by the sensitivity function, which should be decreased in the design. Therefore, the purpose of this paper is to obtain the optimal peak of sensitivity function.

2.2. Unstable Plant Performance Limitation. In this section, the characteristic of the system in combined design and the limitation of the characteristic in an unstable plant are discussed.

Theory 1. Assuming that the open-loop transfer function $K(s)G(s)$ owns unstable poles $p_1, \ldots, p_N$, relative degree $v = n - m > 1$ and the closed-loop system is stable. Then, the sensitivity function of the system satisfies the following equation:

$$\int_0^\infty \ln |S(j\omega)| d\omega = \pi \sum_{i=1}^N \mathrm{Re}(p_i), \tag{9}$$

where n and m are the order of the denominator and numerator, respectively. The proof is seen in [3]. The Bode integral theory is of the linear system, and the design of the linear system will be limited by this integral.

If the controlled plant is stable, the integral is zero, $\int_0^\infty \ln |S(j\omega)| d\omega = 0$. Equation (9) is the logarithm of the sensitivity function, and $S = 1$ is the boundary which decides whether the integral is positive or negative. The sensitivity is above 1 in some frequency band, and then, it will be below 1 in others, which means that the shadow area is fixed in Figure 5. The positive area is larger than the negative are for unstable plants [2].

There, Bode integral is not a real limitation and the negative area is limited between some frequency bands while the positive area is distributed over others small in average. It
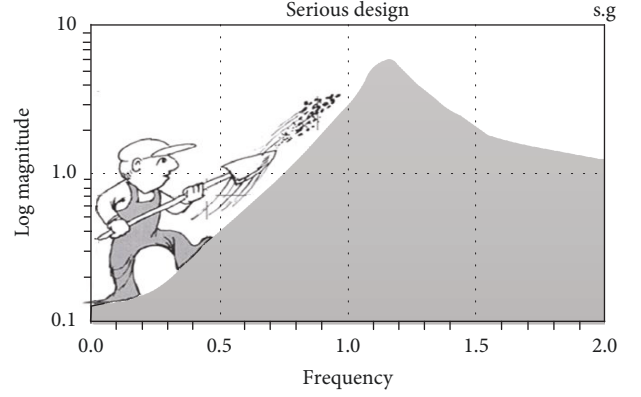

FIGURE 5: Sensitivity reduction at low frequency unavoidably leads to sensitivity increase at higher frequencies.
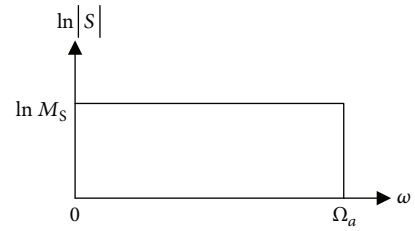

FIGURE 6: The ideal sensitivity function.

means $\ln |s| = \varepsilon$ in the wide-frequency band, and the Nyquist curve of open-loop transfer function is a circle with center $(-1, j0)$ and radius $\approx 1 - \varepsilon$. Therefore, the open-loop transfer function could not decrease in the high-frequency band due to the plant with uncertainty and unmodel dynamics. The bandwidth is generally finite in designing the control system, in which the unmodeled dynamics is described by multiplied uncertainty with its perturbation much less than 1. This means that the characteristics of the system are in coincident with the mathematical model and GK is much less than 1 beyond the bandwidth Ω_a. The outside logarithmic integral is zero in terms of the sensitivity $S = 1/(1 + GK) \approx 1$. Then, the Bode integral is given by

$$\int_0^{\Omega_a} \ln |S(j\omega)| d\omega = 0 \quad \text{(stable plants)}, \tag{10}$$

$$\int_0^{\Omega_a} \ln |S(j\omega)| d\omega = \pi \sum_{i=1}^N \mathrm{Re}(p_i) \quad \text{(unstable plants)}. \tag{11}$$

This is the real constraint with the integral interval Ω_a in application.

From (10) and (11), the integral constrains unstable plants more important than stable plants because the positive area must be larger than the negative area, to be say that M_S is bigger. The minimal M_S is the value of S with rectangular sensitivity characteristics (Figure 6), of which the robustness is optimal. The constraint (11) is fixed for unstable plants, which is the key and the difficulty.

This instance adjusts the weight coefficients to keep the logarithmic sensitivity horizontal flat in bandwidth, which derives the minimal M_s.

There is an unstable pole 6 rad/s and a bandwidth of 40 rad/sec about the fighter jet X-29 in [2], and the optimal sensitivity peak $M_S \approx 1.73$ is derived in terms of (11) [2, 13]. The standard performance is a phase margin of 45° for the fighter jet, but the phase margin of the designed optimal system is 35°, which is not able to improve [2].

Although this is theoretical analysis without the practical system and the constraint of Bode integral is independent of design methods, it can be used to assist the design. The H_∞ control design for the unstable magnetic levitation system is detailed in the following.

3. Linearized Model of the Unstable Magnetic Levitation System

Figure 7 shows a model of the electromagnetic levitation system [10]. For a nominal operating point $z_0 = 4.0 \times 10^{-3}$ m, $i_0 = 3.054$ A with $N = 280$, $m = 15$ kg, $a_m = 1.024 \times 10^{-2}$ m^2, and $R_m = 1.1\,\Omega$; the linearized equations of the levitation system can be given as [14]

$$
\dot{x} = Ax + B_1 w + B_2 u
$$

$$
= \begin{bmatrix} 0 & 1 & 0 \\ 4900 & 0 & -6.4184 \\ 0 & 763.45 & -8.7228 \end{bmatrix} x + \begin{bmatrix} 0 \\ \dfrac{1}{15} \\ 0 \end{bmatrix} w + \begin{bmatrix} 0 \\ 0 \\ 7.9298 \end{bmatrix} u,
$$

$$(12)$$

where the state vector $\mathbf{x}(t) = [z(t)\ \dot{z}(t)\ i(t)]^T$, $x_1 = z$ is the gap between electromagnet and rail, $x_2 = \dot{z}$ is the derivative of $x_1 = z$, and $x_3 = i$ is the current in the coil. w is the perturbation force applied to magnetically levitated train, and u is the voltage in the coil.

4. H_∞ Optimal Performance Design of the Unstable Magnetic Levitation Control System

4.1. H_∞ State Feedback Design. State feedback is the basic control method, and H_∞ state feedback design is the simplest control method in H_∞ control. But state feedback is not a standard problem in H_∞ [6] and it is very different from H_∞ output feedback design, which will be discussed in this section and next section. The relation between the solution of state feedback and H_∞ norm γ is focused by previous articles about state feedback [13] such as bounded real lemma [6] and HJI inequality in a nonlinear problem [10]. However, the real design is not equal to bounded real lemma and HJI inequality. The whole design is that the robustness is restricted by the conditions of solving Riccati equation and Bode integral theory.
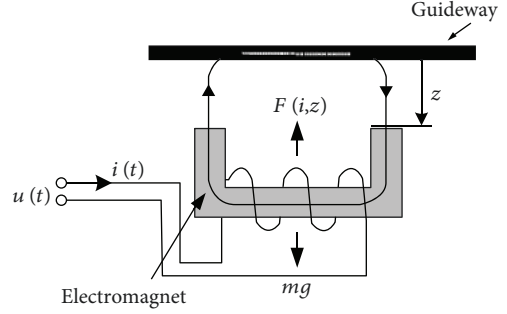

FIGURE 7: Model of the electromagnetic levitation system.

4.1.1. H_∞ Norm γ in State Feedback. The weighted output is first set in H_∞ design and define the output $\mathbf{q}$ as

$$
\mathbf{q} = \mathbf{C}_1 \mathbf{x} + \mathbf{D}_{12}\, u = \begin{bmatrix} \beta_1 & 0 & 0 \\ 0 & \beta_2 & 0 \\ 0 & 0 & \beta_3 \\ 0 & 0 & 0 \end{bmatrix} \begin{bmatrix} x_1 \\ x_2 \\ x_3 \end{bmatrix} + \begin{bmatrix} 0 \\ 0 \\ 0 \\ W_u \end{bmatrix} u,
$$

$$(13)$$

where β_i and W_u are weighted coefficients.

Assume that the transfer function from input w to output $\mathbf{q}$ is T_{qw}, then the goal in H_∞ design is

$$
\left\| T_{qw} \right\|_\infty < \gamma. \tag{14}
$$

The solution of H_∞ state feedback is the central controller in the full information problem, and the Riccati equation is

$$
\mathbf{A}^T\mathbf{P} + \mathbf{P}\mathbf{A} + \mathbf{P}\left(\gamma^{-2}\mathbf{B}_1\mathbf{B}_1^T - \mathbf{B}_2\mathbf{D}^{-1}\mathbf{B}_2^T\right)\mathbf{P} + \mathbf{C}_1^T\mathbf{C}_1 = 0,
$$

$$(15)$$

where $\mathbf{D} = \mathbf{D}_{12}^T\mathbf{D}_{12}$.

Theory 2. Assuming that $(\mathbf{C}_1, \mathbf{A})$ is detectable, there exists a state feedback control law,

$$
u = Kx, \tag{16}
$$

which make the system asymptotic stability and the necessary and sufficient condition of $\|T_{qw}\|_\infty < \gamma$ is that the solution in (4) is greater than or equal to zero. Then,

$$
\mathbf{K} = -\mathbf{D}^{-1}\mathbf{B}_2^T\mathbf{P}. \tag{17}
$$

This theory is a proof result [1, 15].

From Theory 2, the feedback control law (16) could be obtained by solving (15) with MATLAB full information problem function hinffi() if the weight coefficients and γ are given. Therefore, to confirm weight coefficients and γ is the main problem in H_∞ design. But the norm γ in H_∞ state feedback should not be set directly to $\gamma = 1$ because it has a dimension. For example, $\gamma = 1$ means 1 N responds 1 m with

disturbance force and displacement in (12), which requires the index of the system smaller than $1\,\text{m/N} = 10^3\,\text{mm/N}$. This is available for the system with mm dimension, which is an index with $\gamma = \infty$ and is of no use.

So, γ should be confirmed in practical applications and the output $\mathbf{q}$ is the weight product of $\mathbf{x}$ and u in (13). Take the displacement x_1, for example. If the unit of displacement is millimeter and the weight coefficient is 1000, $\gamma = 1$ just means $1\,\text{mm/N}$. So it is appropriate to set $\gamma = 0.1$ or 0.2.

4.1.2. Robustness and Constraints of the State Feedback System. Theoretically, it is possible to minimize γ because H_∞ state feedback design is just to solve Riccati equation (15). But it makes nonsense without any constraints, which may lead to much larger bandwidth. Therefore, it is a complete design to add robustness constraint. There are two problems, unmodeled dynamics and model error under parameter perturbation, in robustness design. The robustness due to unmodeled dynamics could be controlled by the bandwidth and the robustness due to model error is described in terms of the sensitivity S.

It is considerable that H_∞ state feedback is to suppress disturbance signal w in the state feedback scheme and then the bandwidth could be optimized by the LQR method [16].

Together with weighted output (13), the index using the LQR method is given by

$$J = \int_0^\infty \left(\mathbf{x}^\mathrm{T} \mathbf{Q} \mathbf{x} + u^\mathrm{T} \mathbf{R}\, u \right) dt, \tag{18}$$

where $\mathbf{Q}$ and $\mathbf{R}$ are $\mathbf{D}_{12}^\mathrm{T} \mathbf{D}_{12}$ and $\mathbf{D}_{12}^\mathrm{T} \mathbf{D}_{12}$, respectively.

Define the open-loop transfer function of the state feedback system as

$$L(s) = \mathbf{K}_c (s\mathbf{I} - \mathbf{A})^{-1} \mathbf{B}_2. \tag{19}$$

The crossover frequency can be approximated by [3, 16]

$$\omega_c = \frac{\overline{\sigma}[\mathbf{C}_1 \mathbf{B}_2]}{\sqrt{\rho}}, \tag{20}$$

where $\overline{\sigma}$ is the maximum singular value and ρ is $\mathbf{D}_{12}^\mathrm{T} \mathbf{D}_{12}$.

Substituting (12) and (13) into (20),

$$\omega_c = \frac{\overline{\sigma}\left(\begin{pmatrix} \beta_1 & 0 & 0 \\ 0 & \beta_2 & 0 \\ 0 & 0 & \beta_3 \\ 0 & 0 & 0 \end{pmatrix} \begin{bmatrix} 0 \\ 0 \\ 7.9298 \end{bmatrix} \right)}{W_u} = \frac{7.9298\beta_3}{W_u}. \tag{21}$$

The weight coefficients is set as

$$\beta_3 = 1, \\ W_u = 0.12. \tag{22}$$

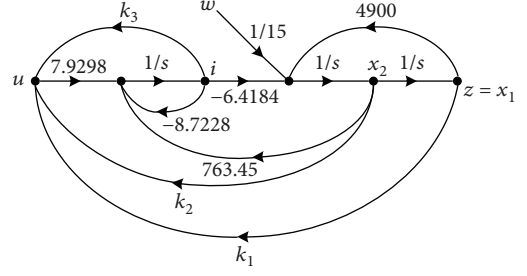

FIGURE 8: Signal flow diagram of the system with state feedback.

And the crossover frequency is

$$\omega_c = 66.08\,\text{rad/sec}, \tag{23}$$

where ω_c is a proper value. The natural frequency of the unstable plant is $\omega_0 = \sqrt{4900} = 70\,\text{rad/sec}$ in terms of (13), and if ω_c and ω_0 is in the same order matching with mathematical model, the system will not be affected by nonmodel high-frequency dynamics, which has an impact on the robustness.

The bandwidth is controlled by weight coefficients using (22), and then, the robustness is up to the sensitivity S. Figure 8 shows signal flow graphic of state feedback.

The plant is the part after the input current of electromagnetic coils, and the controlled input is the current i as shown in Figure 8. The power amplifier and the read and amplifier circuits of all the state variables belong to the controller. Then, the controller equation of the state feedback system in robustness analysis is given by

$$\frac{di}{dt} = -8.7228i + 7.9298(k_3 i + k_2 \dot{z} + k_1 z). \tag{24}$$

The corresponding transfer function is as follows:

$$K(s) = \frac{I(s)}{Z(s)} = \frac{7.9298(k_1 + k_2 s)}{s + (8.7228 - 7.9298k_3)}. \tag{25}$$

And the transfer function of the plant is given by

$$Z(s) = G(s)[I(s) + \alpha W(s)], \tag{26}$$

where

$$G(s) = \frac{-6.4184}{s^2 - 4900}\,\text{m/A}. \tag{27}$$

α is the coefficient of input force to current,

$$\alpha = -\frac{1/15}{6.4184} = -0.0104\,\text{A/N}, \tag{28}$$

where the coupling term (763.45 in (12)) is not included in (27), which is equal to the counter electromotive force caused by the velocity $\dot{z}$ and is calculated combining with feedback

gain k_2. The input sensitivity function of the plant is described by $K(s)$ in (25) and $G(s)$ in (27).

From (27), the plant owns an unstable pole $p_1 = \sqrt{4900} = 70$ and the result in (11) is $\pi \times 70 = 220$ rad/sec, which means that the logarithmic integral of the sensitivity is 220 in terms of Bode integral law. Then, the design's purpose is to make the logarithmic sensitivity same as shown in Figure 6 and minimize M_S by selecting weight coefficient under the constraint $\int_0^{\Omega_a} \ln |S(j\omega)| d\omega = 220$.

4.1.3. Choice of Weight Coefficient and Controller Design. It should be noted that gamma is just a design parameter in designing H_∞ state feedback and the purpose is to achieve the minimum peak M_S of sensitivity function under bandwidth constraint. In terms of 4.1.1, it is reasonable to set $\gamma = 0.2$ and $\beta_1 = 1000$ in this case. In terms of (22) and (27), $\beta_3 = 1$ and $W_u = 0.12$ could be set. The parameter β_2 could be computed by solving (15) under the condition that $S(j\omega)$ of the system mostly approximates the curve in Figure 6.

When $\beta_2 = 25$, a flat curve of sensitivity function $S(j\omega)$ is obtained and all the parameters own proper values. The parameters in this design is as follows:

$$\begin{aligned} \beta_1 &= 1000, \\ \beta_2 &= 25, \\ \beta_3 &= 1. \end{aligned} \tag{29}$$

When $\gamma = 0.2$, using the function hinffi() in MATLAB, the state feedback matrix is obtained by

$$\mathbf{K} = \begin{bmatrix} 30954.68 & 387.86 & -25.40 \end{bmatrix}. \tag{30}$$

4.2. H_∞ Output Feedback Design. Notice that the H_∞ standard problem is an output feedback problem [7]. In this case, if x_1 is used as an output feedback variable, a H_∞ controller is theoretically possible to design. However, if considered from the point of view of engineering practice, the system should add current feedback to suppress various disturbances in the current loop to improve the response characteristic of the current (i.e., electromagnetic force) [3]. First, the current feedback is applied to the system (12), in this example. The equation of the current feedback is combined with formula (30); if the feedback coefficient is set to $k_3 = -25$, then the bandwidth of the current loop is 206.97 rad/sec, see the data in the following formula (32). For system (12), the bandwidth is wide, but it can be realized. Substituting the formula (31) into the (12), the state equation of the system with current feedback is gained as follows:

$$u = k_3 x_3 + v, \tag{31}$$

$$\dot{\mathbf{x}} = \begin{bmatrix} 0 & 1 & 0 \\ 4900 & 0 & -6.4184 \\ 0 & 763.45 & -206.97 \end{bmatrix} \mathbf{x} + \begin{bmatrix} 0 \\ 0 \\ 7.9298 \end{bmatrix} v, \tag{32}$$

$$y = \begin{bmatrix} 1 & 0 & 0 \end{bmatrix} \mathbf{x}.$$

Let us discuss with the most commonly used mixed sensitivity problem in H_∞ control. The following H_∞ optimization problem is alluded to as mixed sensitivity problem:

$$\gamma = \min \left\| \begin{matrix} W_1 S \\ W_2 T \end{matrix} \right\|_\infty \leq 1. \tag{33}$$

In the formula, S refers to the sensitivity of the system, which stands for the system performance. T is the closed-loop transfer function, also known as the complementary sensitivity, and its high frequency is constrained by robust stability. W_1 and W_2 are the corresponding weight functions. The H_∞ controller is designed to ensure the stability of the system, while the performance and robustness correspond to the low-frequency and high-frequency characteristics of the system, so the weight function of S and T is generally considered only from the requirements of the low-frequency and high-frequency segments but not the requirements of the medium-frequency band. But it is dissimilar for the control of the unstable plant, because according to the Nyquist stability criterion, the frequency characteristic of the system is required in encircling counterclockwise the point $-1 + j0$ and this part is exactly in the middle-frequency section. So for unstable plants, weighting functions should take into account the performance characteristics of the middle-frequency band. In addition, the effect of Bode's integral constraint (11) should also be considered in the determination of the weighting function. This limitation is more several if the plant is open-loop unstable.

The rectangular characteristic shown in Figure 6 can be considered as an ideal characteristic for system design. Therefore, the weight function $W_1(s)$ of sensitivity should be determined according to this characteristic. Its amplitude should be kept flat before bandwidth and not be greater than $1/M_S$.

$$|W_1(j\omega)| \leq \frac{1}{M_S}. \tag{34}$$

In the Nyquist diagram shown in Figure 9, notice that the vector **p** from the point -1 to a point on the frequency characteristic curve $K(j\omega)G(j\omega)$ is just the $1 + K(j\omega)G(j\omega)$. So, if $|S|$ is the constant value shown in Figure 6, the frequency characteristic $K(j\omega)G(j\omega)$ of the system at $\omega > 0$ will be the next half circle with $-1 + j0$ point as the center of the circle. Certainly, this is an ideal case. Generally, the Nyquist curve of the unstable plant system will be in the shadow area as shown in Figure 9. This area is composed of two rings with a radius of 0.5 and 0.7, corresponding to $S = 2$ and 1.43, respectively. Due to the constraint of Bode integral, S is not smaller and it is not expected to make S bigger than 2. Figure 2 shows the unit circle, and the crossover frequency ω_c is the point of intersection of KG and unit circle. From the layout of the curves in Figure 9, it can be seen that the nearest distance between KG and the critical point -1 occurs near the crossover frequency ω_c, that is, the sensitivity $S(j\omega)$ reaches the maximum value $S_{\max}$ near ω_c and then gradually attenuates to 1. This case should be considered in the weight function $W_1(s)$.
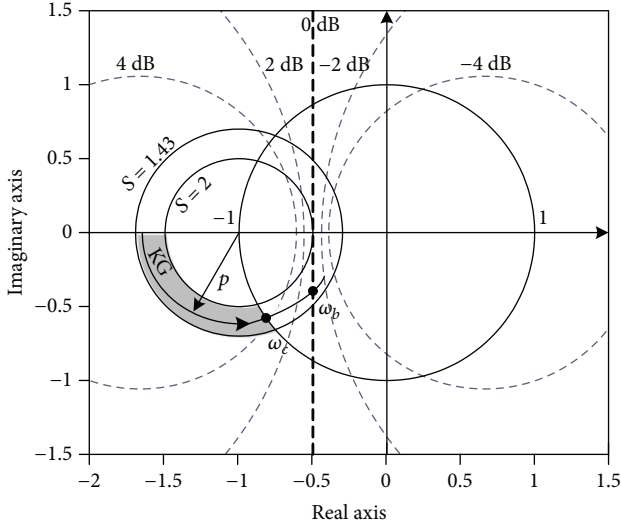
Figure 9: Nyquist locus of $K(j\omega)G(j\omega)$.

Figure 9 shows the readable M circle in the closed-loop magnitude-frequency characteristics. Define the intersection of KG and M = 1 in Figure 9 as ω_b, and the value of closed-loop transfer function $|T(j\omega_b)|$ is 1. After passing the peak and then a long section of frequency, the closed-loop transfer function will decrease to 1, which appears only in unstable plants. The weight function W_2 should be calculated in terms of this.

If the designed control law includes integral law, $K(j\omega)G(j\omega)$ will get into the shallow area in the third quadrant from the second quadrant as shown Figure 9. The shallow area is just up to the performance and Bode integral constraint. The responding sensitivity $S(j\omega)$ increases from zero, and as ω rises, the integral in control law decreases and S increases gradually, which derives the flat curve of S in Figure 6. Because Ω_a could reach 300 rad/sec much larger than the low-frequency band (<10 rad/sec) in second quadrant, the sensitivity could also be approximated in Figure 6. It is applicable for the design of integral control law based on Figures 6 and 9.

If the unstable pole of the magnetic levitation system is 70 rad/sec and the bandwidth is designed in the same order of 70 rad/sec, the mathematical model in (12) is applicable in the work frequency band without nonmodeled dynamics problem in high frequency. Considering this point, the weight function $W_1(s)$ in this case is given by

$$W_1(s) = \frac{0.65 \times 180}{s + 180}, \qquad (35)$$

where it limits the horizontal section by set $M_S = 1/0.65 = 1.538$, which is a good index under Bode integral constraint, to make $|S(j\omega)|$ decrease before 180 rad/sec is set by 180 in (35), which could limit the bandwidth.

The sensitivity design in conventional S/T is to limit bandwidth depending on the weight function T and it is to obtain optimal performance by maximizing the weight function of S. But the weight function W_1 in (35) determines the
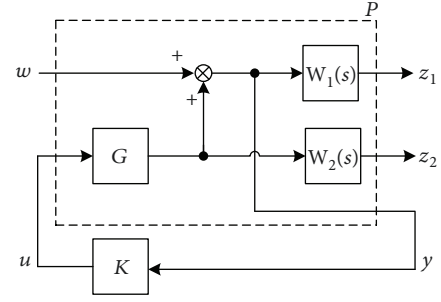
bandwidth in controlling unstable plants. In this paper, the purpose is to use W_1 to control M_S and bandwidth by adjusting W_2.

The weight function W_2 is given by

$$W_2(s) = \frac{s^2}{\rho^2}, \qquad (36)$$

where ρ is an adjustable frequency at the intersection of W_2 and 0 dB. If ρ is large enough in H_∞ design, the solution to (33) is mainly demonstrated by $W_1 S$ in the much-frequency band. Here, the H_∞ optimal solution is all-pass characteristics and if demonstrated by $W_1 S$, $|S|$ will rise up to meet the all-pass characteristics due to $|W_1|$ decreasing when ω is over 180 rad/sec, which make S_{max} lager than the designed M_S. For this case, ρ should be decreased and substituted $W_2 T$ for W_1 to keep all-pass characteristics. That means the optimal solution is composed of $W_1 S$ and $W_2 T$, which makes the sensitivity characteristics flat and meet the bandwidth. The weight function $W_1(s)$ should be fixed to adjust ρ of $W_2(s)$ to make the optimal solution $\gamma \to 1$ in (33).

Figure 10 is the block diagram of the S/T problem in this case. The dashed line is the generalized plant P, G is the system formula (32), W_1 and W_2 are the corresponding weight functions, w and u are the inputs of the generalized plant, and $[z_1 \quad z_2]^T$ and y is the output of the generalized plant. K is the H_∞ controller to be designed. From Figure 10, the generalized plant P in the form of transfer function matrix can be written as

$$P(s) = \begin{bmatrix} P_{11} & P_{12} \\ P_{21} & P_{22} \end{bmatrix} = \begin{bmatrix} W_1 & W_1 G \\ 0 & W_2 G \\ \hline I & G \end{bmatrix}. \qquad (37)$$

It is noted that the P_{12} matrix of the formula (37) does not satisfy the requirement of the rank of the D_{12} matrix. Because take $W_2 G$, for example, the denominator of the plant G is three-order (see (32)), while the numerator of W_2 is the two-order (see (36)). Therefore, a term $(0.001s + 1)$ is added to $W_2(s)$ to make $P_{12}(\infty)$ full column rank. So, the weighting function W_2 is now chosen (38), using (35), (37), and (38), to solve the H_∞ optimization problem. We use MATLAB function hinfsyn() to get $\rho = 185.3248$ when $\gamma = 1.0000$.

Figure 10: Black diagram of the S/T problem.
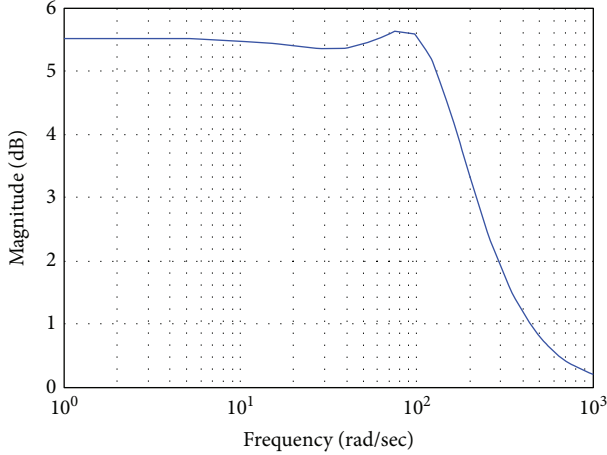
FIGURE 11: The Bode plot of $S(j\omega)$.

FIGURE 12: The disturbance attenuation performance of the system.

The resulting H_∞ controller (after neglecting the high-frequency term 10^{10}) is

$$W_2(s) = \frac{s^2(0.001s + 1)}{\rho^2}, \tag{38}$$

$$K_1(s) = \frac{674833.866(s + 173.1)(s + 155.4)(s + 95.3)}{(s + 951.7)(s + 307.2)(s + 180)}, \tag{39}$$

where the unit of the controller $K_1(s)$ is V/mm and $K_1(0) = 32.873$ V/mm could be achieved in practical application if using mm.

5. Simulation Results

5.1. Results Analysis of H_∞ State Feedback Design

5.1.1. Sensitivity Characteristics. Figure 11 shows the Bode plot of sensitivity function $S(j\omega)$ with the controller (30) in H_∞ state feedback design, and its logarithmic integral equals to 220 in coincident with (11). Although Figure 11 is not rectangular like Figure 6, it can be approximated as a rectangle with average height $M_S = 1.9 = 5.57$ dB. The equivalent bandwidth is $\Omega_a = 342.76$ rad/sec From (11) and Figure 6, the value 1.9 is the minimum sensitivity peak M_S achieved by using state feedback.

5.1.2. The Relation between Disturbance Suppression and Sensitivity. The purpose of H_∞ state feedback is to suppress disturbance so that the norm from w to q is smaller than γ. There, γ is set to be 0.2. The curve 1 is a singular value $\overline{\sigma}[T_{qw}]$ of the last section in Figure 12, and the system norm is $\|T_{qw}\|_\infty = -22.8$ dB $= 0.0724 < 0.2$. Here, **q** is weighted output in design and the real output is displacement variable z of the magnetic levitation system. Due to amplifying $z = x_1$ multiplied by $\beta_1 = 1000$, the curves in Figure 12 are the output $\beta_1 \cdot \overline{\sigma}[T_{zw}]$ multiplied by β_1 and its norm is -31.8 dB and it is $\|T_{zw}\|_\infty = 0.0257 \times 10^{-3}$ m/N, equivalent to that the gap in the magnetic levitation system changes within 0.257 mm under perturbation force of 10 N.
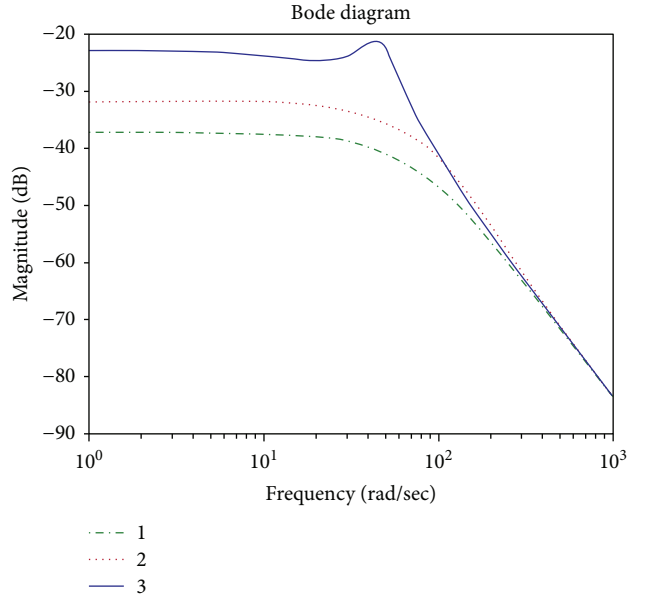
This is the best performance of this system for the relationship of perturbation suppression and sensitivity. The transfer function of disturbance suppression is given by

$$T_{zw}(s) = \frac{G_w(s)}{1 + K(s)G(s)} = G_w(s)S(s), \tag{40}$$

where $G_w(s)$ is the transfer function w from z disturbance input to output as shown in Figure 8,

$$G_w(s) = \frac{1}{15(s^2 - 4900)}. \tag{41}$$

Because $G_w(s)$ is fixed for the given plant, the perturbation suppression is up to sensitivity function. The curve 3 in Figure 12 is amplitude-frequency characteristics of (41), and the difference of curves 2 and 3 is sensitivity characteristics of Figure 4. Therefore, the performance of perturbation suppression is directly up to the designed minimal M_S.

5.2. Result Analysis of H_∞ Output Feedback Design. The sensitivity function $S(j\omega)$ is approximately the same as in Figure 11 under the controller (39) in H_∞ output feedback design, and it is rectangular in practical application, which decreases after the bandwidth. It shows that the area of the rectangle is equivalent in Figure 6 and is the limitation of Bode integral and flat S. The sensitivity function $S(j\omega)$ of H_∞ output feedback design under the controller (39) is the same as Figure 6.

Figure 13 shows the characteristics with the H_∞ controller (39). $\gamma = 1$ in $\overline{\sigma}[T_{zw}]$ is the optimal solution and all-pass characteristics with 0 dB. $|W_1S|$ and $|W_2T|$ are the components of this solution. The closed-loop characteristics $|T(j\omega)|$ and sensitivity $|S(j\omega)|$ are also drawn in Figure 13.
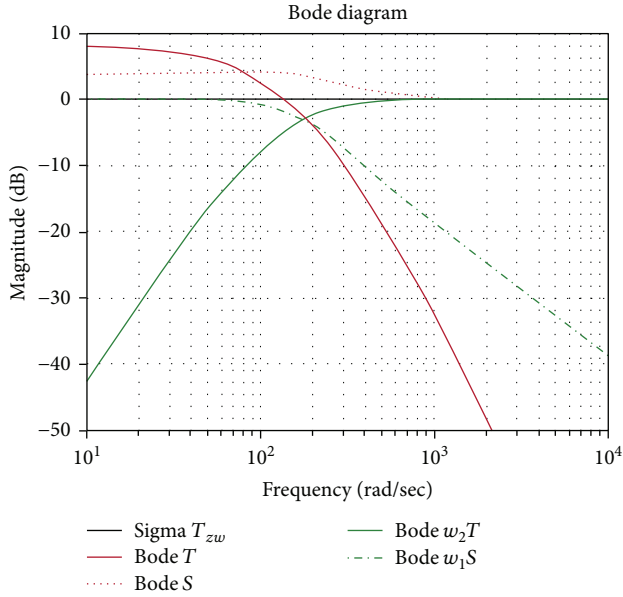
FIGURE 13: Singular value characteristic of the system.

FIGURE 14: Sensitivity function with integral control.

The crossover frequency $|KG|$ of open-loop characteristics is $\omega_c = 80$ rad/sec, and the sensitivity S is flat with peak frequency 90 rad/sec, which is because $|W_2 T|$ rises up to complement $|W_1 S|$. $|W_2 T|$ will shift right with large ρ in W_2 due to that S is increased by the all-pass solution and a large peak comes out after ω_c. This case demonstrates the effect of the adjustable parameter ρ of weight function W_2 in H_∞ optimal design.

The above is designed according to the weight function W_1 of (35), so there is no integral control law in the controller $K_1(s)$. If we need to add integral law, we can add PI to the designed $K_1(s)$. And the obtained controller is

$$K_2(s) = \left(1 + \frac{k_i}{s}\right) K_1(s), \tag{42}$$

where $k_i = 1$ sec^{-1}. Figure 14 shows the sensitivity characteristics with and without integral law, and it can be seen from the figure that the peak of the sensitivity with integral law is a little larger. Increasing k_i, the peak will also be enlarged, even over 6 dB, which causes the robustness of the system to decline. So the good design is to keep the sensitivity flat. The integral law mainly affects the sensitivity when $\omega < 10$ rad/sec. When $\Omega_a \geq 300$ rad/sec, the medium-frequency band is very narrow and the design method above is feasible by Figure 6.

Of course, this kind of sensitivity characteristic with integral control can also be obtained by specifying the weight function in the H_∞ design. For example, when the performance weighting function $W_1(s)$ is as the following

$$W_1(s) = \frac{a}{s}, \tag{43}$$

where a is the design parameter and in this case as shown in Figure 14, a is set as 2 rad/sec. The crossover frequencies ω_{c1} of $|W_1|$ and ω_{c2} of $|W_2|$ are set as $\omega_{c1} = a = 2$ rad/sec
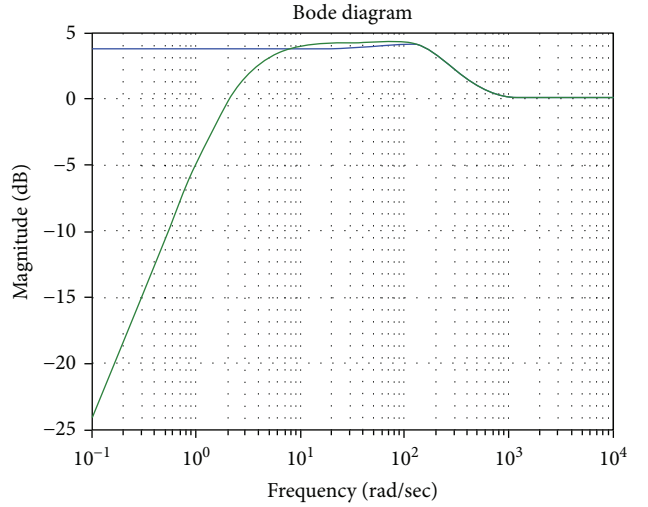
and $\omega_{c2} = \rho = 185.32$ rad/sec. However, in the common H_∞ mixed sensitivity design, the approximate equation $\omega_{c1} \approx \omega_{c2}$ [8] is established when the optimal solution is reached. The large difference between ω_{c1} and ω_{c2} is due to the particular demand for the medium-frequency band in the unstable plant, which demonstrates the difficulty of (43) in general design. This instance is too much between ω_{c1} and ω_{c2} because unstable plants have a particular request for the medium-frequency band. Therefore, the design $W_1(s)$ in (43) is not feasible.

The first kind of unstable plants with a small unstable mode will not be discussed because the difference between ω_{c1} and ω_{c2} is small while achieving the optimal solution. The general S/T design could not achieve the needed performance for the plants with a large unstable mode, and the weight function and H_∞ design could be applied in terms of the flat curve in Figure 6. For the small unstable-mode plants as discussed in Section 1, when achieving optimal solution, ω_{c1} is almost equal to ω_{c2}. However, for the large unstable-mode objects, the traditional design S/T is not able to provide necessary performance and the weight function is needed by the characteristics in Figure 6 to use H_∞ design.

6. Conclusions

This paper presents H_∞ state feedback control and H_∞ output feedback control with respect to the unstable plant, of which the key is the design of weight function or coefficients. In this paper, the weight function or coefficients are obtained subject to the Bode integral constraint, avoiding the repeated attempt. The deficiency in usual designs has been modified, which adds robustness constraint under Bode integral law into H_∞ state feedback control design and points out that the purpose of H_∞ design is to achieve optimal performance by adjusting γ and weight coefficients, not to minimize γ.

The medium-frequency band should be considered to select weight function in H_∞ output feedback design, and together with the magnetic levitation system, it is pointed that the sensitivity function is an adjustable weight function to obtain all-pass and weight sensitivity to control sensitivity peak and bandwidth. Simulation results demonstrate that the H_∞ design of state feedback control and output feedback control subject to the Bode integral constraint could achieve optimal performance.

Data Availability

The data used to support the findings of this study are available from the corresponding author upon request.

Conflicts of Interest

The authors declare that there are no conflicts of interest regarding the publication of this paper.

Acknowledgments

References

[1] F. Meng, X. Chen, Y. Liu, and F. Guo, "Switching control design based on state feedback for unstable plants," *International Journal of Machine Learning and Cybernetics*, vol. 8, no. 6, pp. 2035–2041, 2017.

[2] G. Stein, "Respect the unstable," *IEEE Control Systems Magazine*, vol. 23, no. 4, pp. 12–25, 2003.

[3] F. Meng, X. Chen, Z. Zou, X. Chen, and X. Sha, "Nonlinear H_∞ state feedback control of an electromagnetic suspension system," in *2016 35th Chinese Control Conference (CCC)*, pp. 27–29, Chengdu, China, July 2016.

[4] X. Jiang, X. Tian, T. Zhang, and W. Zhang, "Quadratic stabilizability and H_∞ control of linear discrete-time stochastic uncertain systems," *Asian Journal of Control*, vol. 19, no. 1, pp. 35–46, 2017.

[5] Y.-p. Luo, F. Deng, B.-f. Zhou, X. Luo, and H. Liu, "H_∞ non-fragile synchronous guaranteed control of uncertainty complex dynamic network with time-varying delay," *Asian Journal of Control*, vol. 18, no. 6, pp. 2109–2121, 2016.

[6] J. C. Doyle, K. Glover, P. P. Khargonekar, and B. A. Francis, "State-space solutions to standard H_2 and H_∞ control problems," *IEEE Transactions on Automatic Control*, vol. 34, no. 8, pp. 831–847, 1989.

[7] N. Olgac and A. S. Kammer, "Stabilisation of open-loop unstable plants under feedback control with distributed delays," *IET Control Theory & Applications*, vol. 8, no. 10, pp. 813–820, 2014.

[8] M. G. Safonov and R. Y. Chiang, "CACSD using the state-space L_∞ theory—a design example," *IEEE Transactions on Automatic Control*, vol. 33, no. 5, pp. 477–479, 1988.

[9] A. Bittar and R. Moura Sales, "H_2 and H_∞ control for maglev vehicles," *IEEE Control Systems*, vol. 18, no. 4, pp. 18–25, 1998.

[10] P. K. Sinha and A. N. Pechev, "Nonlinear H_∞ controllers for electromagnetic suspension systems," *IEEE Transactions on Automatic Control*, vol. 49, no. 4, pp. 563–568, 2004.

[11] K. J. Åström, H. Panagopoulos, and T. Hägglund, "Design of PI controllers based on non–convex optimization," *Automatica*, vol. 34, no. 5, pp. 585–601, 1998.

[12] E. Vidal-Idiarte, L. Martinez-Salamero, H. Valderrama-Blavi, F. Guinjoan, and J. Maixe, "Analysis and design of H_2/H_∞ control of nonminimum phase-switching converters," *IEEE Transactions on Circuits and Systems I: Fundamental Theory and Applications*, vol. 50, no. 10, pp. 1316–1323, 2003.

[13] M. Wang and J. Zhao, "L_2-gain analysis and control synthesis for a class of uncertain switched nonlinear systems," *Acta Automatica Sinica*, vol. 35, no. 11, pp. 1459–1464, 2009.

[14] F. W. Meng, Z. He, Y. Wang, and D. Zhou, "Linearization of a nonlinear system," *Electric Machines and Control*, vol. 12, no. 1, pp. 89–92, 2008.

[15] A. J. van der Schaft, "L_2-gain analysis of nonlinear systems and nonlinear state feedback H_∞ control," *IEEE Transactions on Automatic Control*, vol. 37, no. 6, pp. 770–784, 1992.

[16] J. Doyle and G. Stein, "Multivariable feedback design: concepts for a classical/modern synthesis," *IEEE Transactions on Automatic Control*, vol. 26, no. 1, pp. 4–16, 1981.